

Electron spin resonance of Nd^{3+} and Yb^{3+} in $\text{CeFe}_4\text{P}_{12}$

G. B. Martins, M. A. Pires, G. E. Barberis, and C. Rettori

Instituto de Física, Universidade Estadual de Campinas (UNICAMP), Campinas 13081-970, São Paulo, Brazil

M. S. Torikachvili

Department of Physics, San Diego State University, San Diego, California 92182

(Received 1 July 1994)

Electron spin resonance experiments, at low temperature (1.6–4.2 K), of Nd^{3+} and Yb^{3+} in the small-gap semiconductor $\text{CeFe}_4\text{P}_{12}$ show cubic-crystal-field $\Gamma_8^{(2)}$ and Γ_6 ground states, respectively. The sign and ratio between the fourth and sixth order cubic-crystal-field parameters were found to be in agreement with those previously determined for Dy^{3+} and Er^{3+} in the same compound. Dysonian resonance line shapes, characteristic of metallic hosts, were observed in all our experiments. However, no exchange interaction effects between the localized rare-earth magnetic moment and conduction electrons were detected. This result supports the idea that in $\text{CeFe}_4\text{P}_{12}$ there is a strong 4*f*-conduction-electron hybridization with an open gap in the density of states at the Fermi level.

I. INTRODUCTION

The compounds $R\text{Fe}_4\text{P}_{12}$ ($R=\text{La}, \text{Ce}, \text{Pr}, \text{Nd}, \text{Eu}$) are cubic¹ and $\text{CeFe}_4\text{P}_{12}$ is the only one that shows a semiconductorlike temperature dependence of the resistivity.^{2,3} Furthermore, $\text{CeFe}_4\text{P}_{12}$ shows an almost temperature-independent magnetic susceptibility and a smaller lattice parameter than that expected for trivalent Ce. These properties suggest that either the Ce atoms are nearly tetravalent or there is a strong 4*f*-conduction-electron hybridization with an open gap in the density of states at the Fermi level.^{2,3} However, recent resistivity measurements⁴ showed metallic behavior ($d\rho/dT > 0$) in $\text{ThFe}_4\text{P}_{12}$. Since in this compound Th is likely to be tetravalent, 4*f*-conduction-electron hybridization seems to be the mechanism responsible for the observed properties in $\text{CeFe}_4\text{P}_{12}$.

It is known that electron spin resonance (ESR) experiments on dilute magnetic rare earths in metallic compounds can give valuable information about the local crystal field (CF) and exchange interaction between the localized magnetic moment and conduction electrons.^{5,6} Hence the aim of this work is to study the ESR spectra of Nd^{3+} and Yb^{3+} in $\text{CeFe}_4\text{P}_{12}$ in order to contribute to a better understanding of the electronic properties of this compound.

II. EXPERIMENT

Single crystals of $\text{Ce}_{1-x}\text{R}_x\text{Fe}_4\text{P}_{12}$ ($R=\text{Nd}, \text{Yb}$) with $x \approx 0.002$ were grown in a molten Sn flux.³ Typical crystal dimensions were about 2 mm, and the samples showed clearly the natural crystallographic growing faces. These faces were used to orient the crystals in the resonant cavity in order to obtain the angular dependence of the spectra. The ESR experiments were carried out in a conventional X-band ESR Varian *E*-line spectrometer using a

liquid helium (1.6–4.2 K) tail quartz Dewar adapted to a room temperature TE₁₀₂ (100 kHz) cavity.

III. RESULTS AND ANALYSIS

A. $\text{Ce}_{1-x}\text{Nd}_x\text{Fe}_4\text{P}_{12}$

The ESR spectra of Nd^{3+} in $\text{CeFe}_4\text{P}_{12}$ at liquid helium temperature show two main anisotropic resonances. The temperature dependence of the intensity, down to 1.6 K, indicates that both resonances belong to the ground state. Figures 1 and 2 show, respectively, the *g* value and relative intensity anisotropies for both resonances when the magnetic field is rotated in a (110) plane. Figures 3

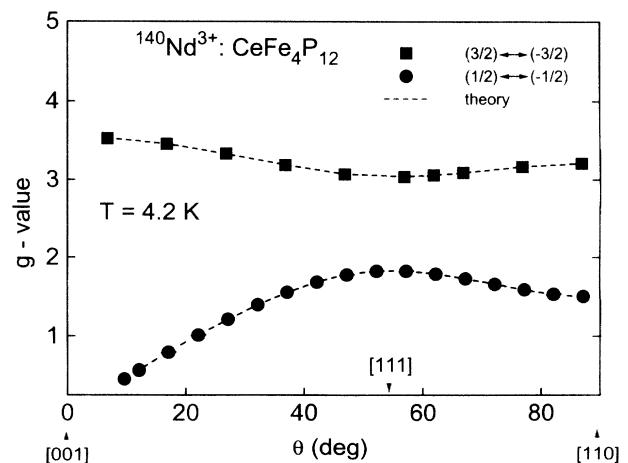


FIG. 1. *g* value anisotropy for the two observed resonances of $^{140}\text{Nd}^{3+}$ in $\text{CeFe}_4\text{P}_{12}$. The dashed lines are the theoretical fittings for the two Kramers doublets of the $\Gamma_8^{(2)}$ quartet. The obtained parameters were (see text) $g_J = 0.7335(5)$, $x = -0.566(5)$, and $W \leq -0.100(5)$.

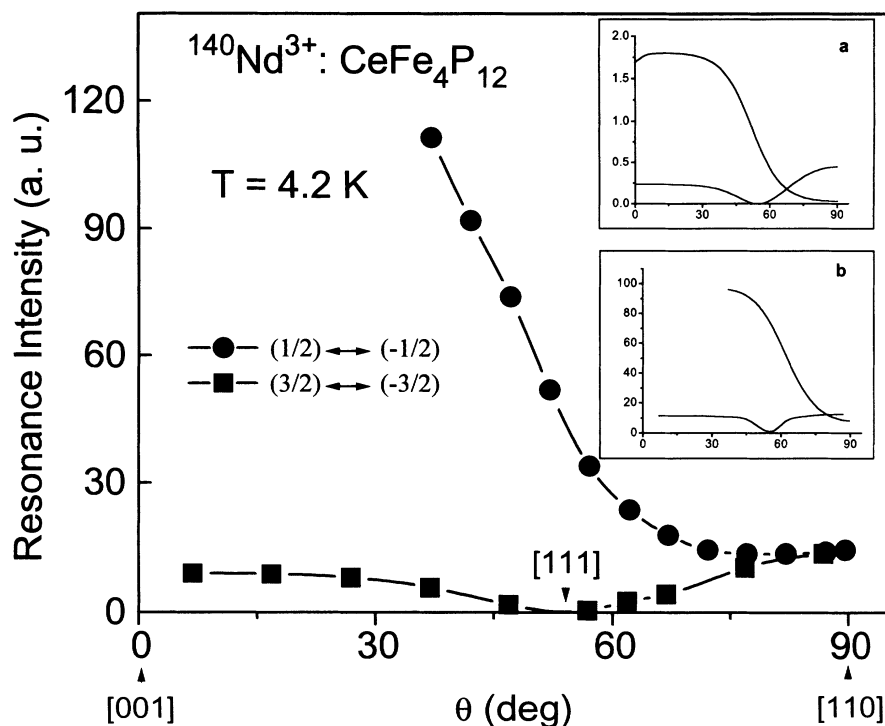


FIG. 2. Relative intensity anisotropy for the two resonances of Fig. 1. See text for a description of insets *a* and *b*.

and 4 correspond to the spectra observed for one of them at 4.2 K for two different orientations of the external magnetic field. The resonances show Dysonian line shape^{7,8} characteristic of conducting hosts. The spectrum consists of 17 lines corresponding to the various Nd^{3+} isotopes; $^{140}\text{Nd}^{3+}$ ($I = 0$, 79.4%), $^{143}\text{Nd}^{3+}$ ($I = 7/2$, 12.3%), and $^{145}\text{Nd}^{3+}$ ($I = 7/2$, 8.3%). The hyperfine splittings for both isotopes with $I = 7/2$ were found to be anisotropic. Figures 5 and 6 show this anisotropy in the (110) plane for both isotopes and for angles where the hyperfine splittings could be clearly observed.

It is reasonable to believe that the Nd atoms replace the Ce atoms in the lattice; thus the site symmetry is expected to be cubic for the Nd^{3+} ions. The Hamiltonian describing the energy levels within a manifold of angular momentum J in the presence of an external magnetic

field and a crystal field of cubic point symmetry is given by⁹

$$\mathcal{H} = g_J \mu_B \vec{H} \cdot \vec{J} + \beta A_4 \langle r^4 \rangle \left[O_4^0(\vec{J}) + 5 O_4^4(\vec{J}) \right] + \gamma A_6 \langle r^6 \rangle \left[O_6^0(\vec{J}) - 21 O_6^4(\vec{J}) \right], \quad (1)$$

where the first term is the Zeeman interaction and the second and third terms the cubic crystal field; β and γ are reduced matrix elements, $A_4 \langle r^4 \rangle$ and $A_6 \langle r^6 \rangle$ are the fourth and sixth order crystalline field parameters, and O_n^m are the Stevens equivalent operators.⁹

Following Lea, Leask, and Wolf¹⁰

$$\mathcal{H} = g_J \mu_B \vec{H} \cdot \vec{J} + W \left[x \frac{O_4}{F_4} + (1 - |x|) \frac{O_6}{F_6} \right], \quad (2)$$

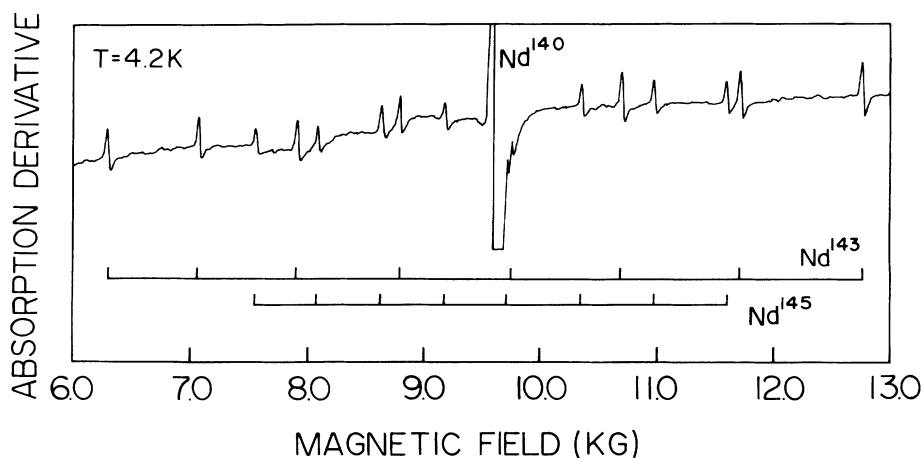


FIG. 3. ESR spectrum of Nd^{3+} in $\text{CeFe}_4\text{P}_{12}$ for an angle of 15° between the external magnetic field and the [001] direction, in the (110) plane.

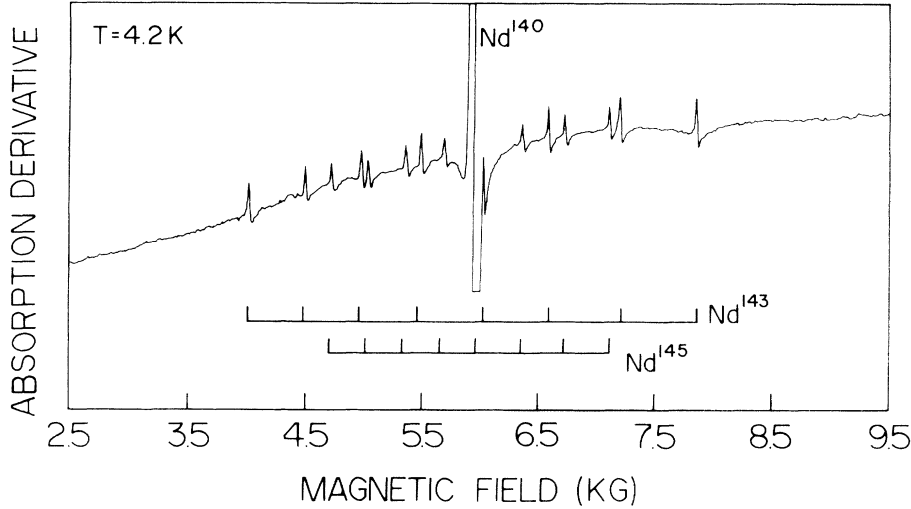


FIG. 4. ESR spectrum of Nd^{3+} in $\text{CeFe}_4\text{P}_{12}$ for an angle of 25° between the external magnetic field and the $[001]$ direction, in the (110) plane.

where

$$\begin{aligned}\beta A_4 \langle r^4 \rangle F_4 &= Wx, \\ \gamma A_6 \langle r^6 \rangle F_6 &= W(1 - |x|), \\ O_4 &= O_4^0(\vec{J}) + 5O_4^4(\vec{J}), \\ O_6 &= O_6^0(\vec{J}) - 21O_6^4(\vec{J}).\end{aligned}$$

Since the observed resonances are anisotropic and both belong to the ground state, they should come from transitions within the Zeeman levels of one of the two $\Gamma_8^{(i)}$ quartets that result from the splitting of the free Nd^{3+} ($4f^3$, $^4I_{9/2}$) ion ground state in the cubic crystal field.⁹ The best fit of Eq. (2) to the experimental data of Fig. 1, taking into consideration the exact diagonalization of the 10×10 ($J = 9/2$) energy matrix when the magnetic field is rotated in a (110) plane, gives $g_J = 0.7335(5)$, $x = -0.566(5)$, and $W \leq -0.100(5)$. According to these

values the ground state of Nd^{3+} in $\text{CeFe}_4\text{P}_{12}$ is the $\Gamma_8^{(2)}$ quartet, and the observed resonances correspond to the transitions within the Kramers doublets. However, the free Nd^{3+} ion Landé factor, $g_J = 8/11$, is smaller than that found above. It is known that the spin-orbit coupling can admix different Russel-Saunders (RS) multiplets with the same total angular momentum J and give rise to a new Landé g_J factor for each multiplet. This effect is important for Nd^{3+} and Pr^{3+} , because for these ions the first excited RS multiplet (with the same J as that of the ground state multiplet) lies closer than in any other rare-earth ion. For Nd^{3+} the first $J = 9/2$ excited multiplet ($^2H_{9/2}$) lies¹¹ at $\sim 13\,000\text{ cm}^{-1}$. Using the intermediate coupling approach¹² and including all RS excited multiplets, a new Landé factor can be calculated:¹³

$$g_J^{ic} = \sum_{L,S} |\xi_{L,S}|^2 g_J^{L,S}, \quad (3)$$

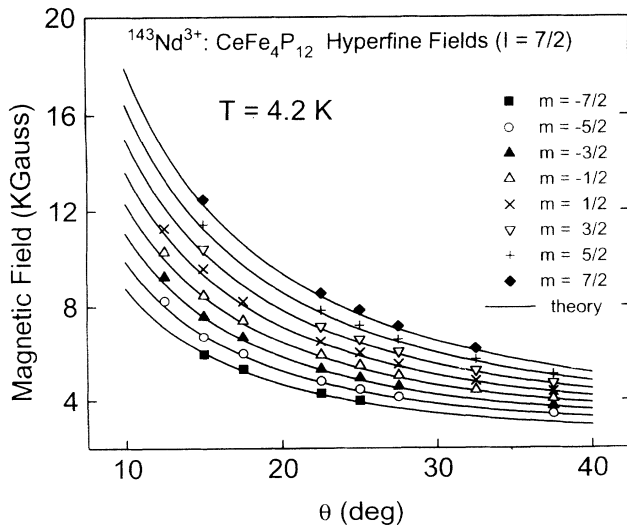


FIG. 5. Resonance fields of the hyperfine lines for the $^{143}\text{Nd}^{3+}$ isotope from 10° to 40° away from the $[001]$ direction. The continuous lines are the theoretically calculated fields for resonances (see text).

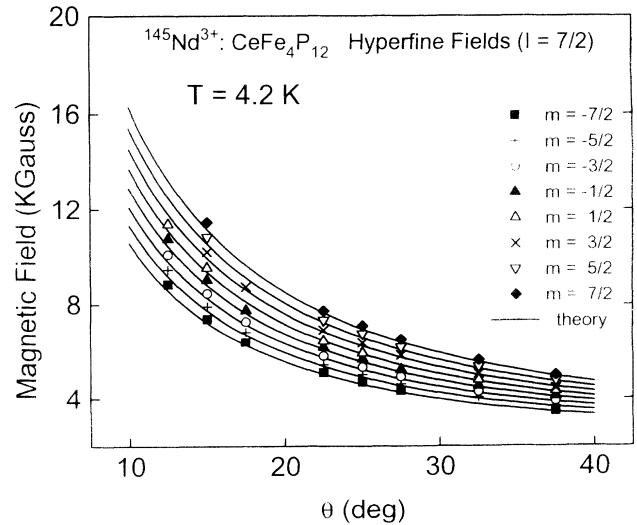


FIG. 6. Resonance fields of the hyperfine lines for the $^{145}\text{Nd}^{3+}$ isotope from 10° to 40° away from the $[001]$ direction. The continuous lines are the theoretically calculated fields for resonances (see text).

where

$$g_J^{L,S} = \frac{3}{2} + \frac{S(S+1) - L(L+1)}{2J(J+1)}$$

and the intermediate coupling wave functions are given by

$$|JM_J\rangle = \sum_{L,S} \xi_{L,S} |LSJM_J\rangle.$$

Using in Eq. (3) the values of $\xi_{L,S}$ calculated by Wybourne¹⁴ for the ground multiplet of Nd³⁺ we obtain $g_J^{ic} = 0.7332$, which is very close to that obtained from the fitting of our experimental data.

The inset *a* in Fig. 2 shows the angular dependence of the square of the magnetic dipole matrix elements for the two Kramers doublets of the $\Gamma_8^{(2)}$ ground state. Even though this angular dependence seems to be the appropriate one, their relative values, mainly near the [110] direction, disagree with the experimental data. Since transitions between levels of different Kramers doublets are allowed and are easily broadened by crystal field inhomogeneities it is expected that they may affect the equilibrium population of the Kramers doublets and in turn the absorbed microwave power of the observed transitions. Taking into account all the possible transitions within the $\Gamma_8^{(2)}$ multiplet, we simulated the absorbed power of the transitions for both Kramers doublets. The inset *b* shows that this calculation leads to relative intensities which are closer to the experimental data, in spite of the unknown actual crystal field inhomogeneous line broadening and spontaneous transition probabilities for the various transitions.

Owing to the strong anisotropy of the spectra (*g* value, intensity, and hyperfine splittings) we were able to follow the hyperfine splittings of the ¹⁴³Nd³⁺ and ¹⁴⁵Nd³⁺ isotopes only within a few degrees of the [001] direction in the (110) plane (see Fig. 5 and Fig. 6). Since the crystal field parameters (*x* and *W*) given above guarantee that the $\Gamma_8^{(2)}$ ground state is quite isolated, we shall use for simplicity the spin-Hamiltonian approach with an effective spin $\tilde{S} = 3/2$ for the analysis of the hyperfine lines. The spin Hamiltonian describing the hyperfine and Zeeman interactions in a $\Gamma_8^{(i)}$ quartet can be written as follows:⁹

$$\begin{aligned} \mathcal{H} = & ag_J \mu_B \vec{H} \cdot \vec{S} + a\mathcal{A}_J \vec{S} \cdot \vec{I} \\ & + bg_J \mu_B (S_x^3 H_x + S_y^3 H_y + S_z^3 H_z) \\ & + b\mathcal{A}_J (S_x^3 I_x + S_y^3 I_y + S_z^3 I_z), \end{aligned} \quad (4)$$

where

$$a = -\frac{P}{12} + \frac{9Q}{4},$$

$$b = \frac{P}{3} - Q,$$

and

$$\begin{aligned} P &= \langle 3/2 | J_z | 3/2 \rangle, \\ Q &= \langle 1/2 | J_z | 1/2 \rangle. \end{aligned} \quad (5)$$

For an effective electronic spin $\tilde{S} = 3/2$ and nuclear spin $I = 7/2$, Eq. (4) gives a 32×32 matrix dependent on *P*, *Q*, and \mathcal{A}_J . Using in Eq. (5) the $\Gamma_8^{(2)}$ wave functions corresponding to $x = -0.566$ obtained above, we calculate $P = 2.4145$ and $Q = -0.0791$. With these values we can calculate the resonance fields of the hyperfine lines for each isotope by diagonalizing the 32×32 matrix with \mathcal{A}_J being the only adjustable parameter. The best fit, shown in Fig. 5 and Fig. 6, gives $|\mathcal{A}_J| = 248(30)$ MHz and $|\mathcal{A}_J| = 155(20)$ MHz. These values are in good agreement with those measured in insulators.⁹

We want to mention that we have also done a perturbation analysis to second order in the hyperfine coupling for the [001] and [111] directions.¹⁵ To first order there is no difference in hyperfine splittings between these two directions [actually the hyperfine splitting is isotropic in the (110) plane to first order]. However, there is an angular dependence in the second order term. In our case for the [001] direction the second order contribution almost triples the hyperfine splitting in comparison with that of the first order calculation, while for the [111] direction it introduces almost no change. It is also easy to verify¹⁵ that the second order term along the [001] direction becomes important for small values of *Q* ($\sim 10^{-2}$). A small value of *Q* implies a small *g* value along the [001] direction for the $1/2 \longleftrightarrow -1/2$ transition [see Eq. (5) and Fig. 1].

B. Ce_{1-x}Yb_xFe₄P₁₂

Figure 7 shows the spectrum corresponding to ¹⁷⁰Yb³⁺ ($I = 0, 69.9\%$), ¹⁷¹Yb³⁺ ($I = 1/2, 14.3\%$), and ¹⁷³Yb³⁺ ($I = 5/2, 16.1\%$) isotopes. The resonances are isotropic and also show Dysonian line shapes. The measured *g* value of 2.58 ± 0.01 and the temperature dependence of the intensity indicate that the resonance corresponds to a Γ_6 ground state ($g_{\Gamma_6} = 2.667$). The measured hyperfine constants for ¹⁷¹Yb³⁺ and ¹⁷³Yb³⁺ are $|\mathcal{A}_J| = 704(15)$ MHz and $|\mathcal{A}_J| = 190(4)$ MHz, respectively.

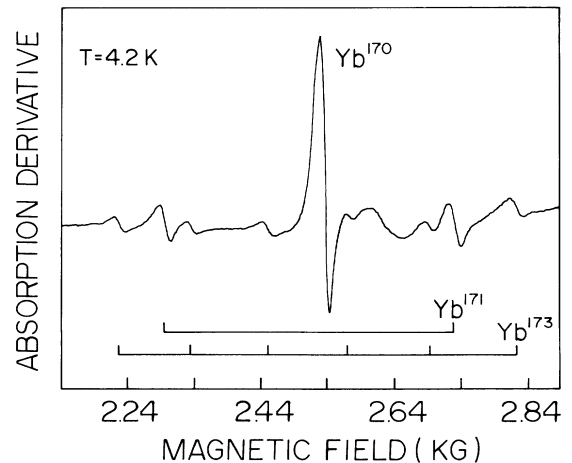


FIG. 7. ESR spectrum of Yb³⁺ in CeFe₄P₁₂.

TABLE I. Rare-earths hyperfine constants $|A_J|$ (MHz) in $\text{CeFe}_4\text{P}_{12}$.

	Nd^{3+}		Dy^{3+}		Er^{3+}	Yb^{3+}	
Isotope	143	145	161	163	167	171	173
Ours	248(30)	155(20)	110.2(9)	155.9(9)	124.9(8)	704(15)	190(4)
Ref. 9	220.3(2)	136.9(1)	109.5(22)	152.4(30)	125.3(12)	887.2(15)	243.3(4)

IV. DISCUSSION

This work along with our previous paper¹⁶ shows that the rare earths (Nd^{3+} , Gd^{3+} , Dy^{3+} , Er^{3+} , and Yb^{3+}) occupy cubic sites in $\text{CeFe}_4\text{P}_{12}$, probably replacing the Ce atoms. All the rare-earth ESR data are consistent with a negative fourth order crystal field parameter and a positive sixth order crystal field parameter. In particular the ratio $A_4\langle r^4 \rangle / A_6\langle r^6 \rangle$ was found to be ≈ -9 for Er^{3+} and ≈ -7.5 for Nd^{3+} , where the difference can be easily accounted for by the difference in $\langle r^4 \rangle / \langle r^6 \rangle$ ratios¹⁷ between Er^{3+} and Nd^{3+} . This confirms the customary idea that the host electric crystal field is not significantly modified by the substitution of different rare earths.

Table I shows the magnetic hyperfine constant A_J for all measured rare-earth isotopes in $\text{CeFe}_4\text{P}_{12}$. It is interesting to note that, except for Yb^{3+} isotopes, the values obtained are consistent with those found in other insulating⁹ hosts. The reason for the strong reduction ($\sim 20\%$) observed in the hyperfine constant for both Yb^{3+} isotopes is not clear to us at the moment. However, it is worth noting that Yb is often found to show Kondo, intermediate valence, and heavy fermion behavior, in a variety of compounds, indicative of strong $4f$ (Yb) character for the conduction electrons at the Fermi level. Thus the $4f$ (Ce) conduction-electron hybridization, responsible for an open gap at the Fermi level, probably affects the hyperfine field at the Yb^{3+} nucleus and is therefore responsible for the observed reduction in the hyperfine constants.

V. CONCLUSIONS

In summary, our ESR experiments demonstrate that rare earths show localized $4f$ magnetic moments in $\text{CeFe}_4\text{P}_{12}$ and occupy sites of cubic symmetry, probably substituting for the Ce^{3+} ions. The electric crystal field does not seem to be affected by the substitution of different rare earths. The magnetic hyperfine interaction, except for Yb^{3+} , is found to be the same as those measured in insulators, with no observable contribution from conduction electrons.¹⁸ This and the absence of g shift (relative to insulating hosts) and thermal broadening of the line (Korringa relaxation) for all rare earths are consistent with the existence of a gap in the density of states at the Fermi level, supporting the idea that there is a strong $4f$ (Ce) conduction-electron hybridization in $\text{CeFe}_4\text{P}_{12}$. Clearly, further theoretical work is needed in order to see if this hybridization can also explain the observed reduction in the Yb^{3+} hyperfine constants.

ACKNOWLEDGMENTS

The support of FAPESP (Fundação de Amparo à Pesquisa do Estado de São Paulo) and CNPq for the research performed at UNICAMP and the support of the National Science Foundation under Grant No. INT-8815391e for the research performed at SDSU are gratefully acknowledged.

¹ W. Jeitschko and D. J. Braun, *Acta Crystallogr. Sect. B* **33**, 3401 (1977).

² M. S. Torikachvili, M. B. Maple, and G. P. Meisner, in *Proceedings of the 17th International Conference on Low Temperature Physics (LT-17)*, edited by U. Eckern (Elsevier, Amsterdam, 1984).

³ G. P. Meisner, M. S. Torikachvili, K. N. Yang, M. B. Maple, and R. P. Guertin, *J. Appl. Phys.* **57**, 3073 (1985).

⁴ M. S. Torikachvili, J. W. Chen, Y. Dalichaouch, R. P. Guertin, M. W. McElfresh, C. Rossel, M. B. Maple, and G. P. Meisner, *Phys. Rev. B* **36**, 8660 (1987).

⁵ D. Davidov, C. Rettori, R. Orbach, A. Dixon, and E. P. Chock, *Phys. Rev. B* **11**, 3546 (1975).

⁶ D. Davidov, E. Buckner, L. W. Rupp, L. D. Longonitti, and C. Rettori, *Phys. Rev. B* **9**, 2879 (1974).

⁷ G. Feher and A. K. Kipp, *Phys. Rev.* **98**, 337 (1955).

⁸ F. J. Dyson, *Phys. Rev.* **98**, 349 (1955).

⁹ A. Abragam and B. Bleaney, *Electron Paramagnetic Resonance of Transition Ions* (Oxford University Press, Oxford, 1970).

¹⁰ K. R. Lea, M. J. M. Leask, and W. P. Wolf, *J. Phys. Chem. Solids* **23**, 1381 (1962).

¹¹ S. Hufner, *Optical Properties of Transparent Rare Earth Compounds* (Academic Press, New York, 1978), p. 19.

¹² B. R. Judd, *Proc. Phys. Soc. London Sect. A* **69**, 157 (1956).

¹³ Y. Ayant and Elie Belorizky, *C. R. Acad. Sci.* **259**, 3748 (1964).

¹⁴ B. G. Wybourne, *J. Chem. Phys.* **34**, 279 (1961).

¹⁵ E. Belorizky, Y. Ayant, D. Descamps, and Y. M. D'Aubigné, *J. Physique* **27**, 313 (1966).

¹⁶ R. N. Mesquita, G. E. Barberis, C. Rettori, M. S. Torikachvili, and M. B. Maple, *Solid State Commun.* **74**, 1047 (1990).

¹⁷ A. J. Freeman and R. E. Watson, *Phys. Rev.* **127**, 6 (1962).

¹⁸ L. J. Tao, D. Davidov, R. Orbach, and E. P. Chock, *Phys. Rev. B* **4**, 5 (1971); D. Davidov, R. Orbach, C. Rettori, D. Shattiel, and L. J. Tao, *Phys. Lett.* **37A**, 361 (1971); E. P. Chock, D. Davidov, R. Orbach, C. Rettori, and L. J. Tao, *Phys. Rev. B* **5**, 2735 (1972).